Hybrid giant lipid vesicles incorporating a PMMA-based copolymer

Ylenia Miele, Anne-Françoise Mingotaud, Enrico Caruso, Miryam Malacarne, Lorella Izzo, Barbara Lonetti, Federico Rossi

Hybrid giant lipid vesicles incorporating a PMMA-based copolymer

Ylenia Miele[a], *Anne-Françoise Mingotaud*[b], *Enrico Caruso*[c], *Miryam C. Malacarne*[c], *Lorella Izzo**[c], *Barbara Lonetti**[b], *Federico Rossi*[d]

[a] Department of Chemistry and Biology, University of Salerno, Via Giovanni Paolo II, 132, 84084 Fisciano – Italy.

[b] Laboratoire des IMRCP, Université de Toulouse, CNRS UMR 5623, Université Toulouse III - Paul Sabatier, 118 Rte de Narbonne, F-31062 Toulouse cedex 9 – France.

[c] Dipartimento di Biotecnologie e Scienze della Vita, Università degli Studi dell'Insubria, via J. H. Dunant, 3, 21100 Varese – Italy.

[d] Department of Earth, Environmental and Physical Sciences – DEEP Sciences – Pian dei Mantellini 44, 53100 Siena – Italy.

* Corresponding Author: L.I. lorella.izzo@uninsubria.it

B.L lonetti@chimie.ups-tlse.fr

STATISTICAL SUMMARY

Words: 6494

Figures/Tables: 5

HIGHLIGHTS

- Methacrylate based polymer is mixed with a lipid to produce giant vesicles
- Electroformation is not a suitable method to obtain such hybrid systems
- Phase transfer method is used to obtain hybrid giant vesicles
- Phase transfer method useful when the polymer has a relatively high T_g

ABSTRACT

Background

In recent years, there has been a growing interest in the formation of copolymer-lipid hybrid self-assemblies, which allow combining and improving the main features of pure lipid-based and copolymer-based systems known for their potential applications in the biomedical field. As the most common method used to obtain giant vesicles is electroformation, most systems so far used low T_g polymers for their flexibility at room temperature.

Methods

Copolymers used in the hybrid vesicles have been synthesized by a modified version of the ATRP, namely the Activators ReGenerated by Electron Transfer ATRP and characterized by NMR and DSC. Giant hybrid vesicles have been obtained using electroformation and droplet transfer method. Confocal fluorescence microscopy was used to image the vesicles.

Results

Electroformation enabled to obtain hybrid vesicles in a narrow range of compositions (15 mol % was the maximum copolymer content). This range could be extended by the use of a droplet transfer method, which enabled obtaining hybrid vesicles incorporating a methacrylate-based polymer in a wide range of compositions. Proof of the hybrid composition was obtained by fluorescence microscopy using labelled lipids and copolymers.

Conclusions

This work describes for the first time, to the best of our knowledge, the formation of giant hybrid polymer/lipid vesicles formed with such a content of a polymethylmethacrylate copolymer, the glass temperature of which is above room temperature.

General Significance

This work shows that polymer structures, more complex than the ones mostly employed, can be possibly included in giant hybrid vesicles by using the droplet transfer method. This will give easier access to functionalized and stimuli-responsive giant vesicles and to systems exhibiting a tunable permeability, these systems being relevant for biological and technological applications.

KEYWORDS liposomes; polymersomes; hybrid GUVs; self-assembly; surfactant; polymer; phase transfer method

1. INTRODUCTION

Liposomes and polymersomes are self-assembled vesicles formed by lipids and copolymers respectively and characterized by the presence of a hydrophobic double layer delimitating an internal water pool. Their structure allows the encapsulation of both hydrophobic and hydrophilic components with high loading efficiency, which mainly boosted the research in applications related to drug delivery [1–4]. Besides, the last 10 years of research witnessed a growing interest in polymersomes used as reactors [5]. For this particular application, the low bilayer permeability of the high molecular weight constituents represents a drawback. Block copolymers forming intrinsically permeable polymersomes [6,7], polymersomes whose permeability can be modulated by a stimulus, i.e. pH [8], light [9], CO_2 [10], and self-adaptive polymersomes [5] have been proposed. A further, less explored possibility is the use of hybrid lipid/polymer vesicles, which could exploit the complementary properties of liposomes and polymersomes, i.e. biocompatibility, biodegradability and permeability of the former and high mechanical stability and chemical versatility of the latter. These hybrid vesicles have higher permeability to small dyes like carboxyfluorescein or calcein with respect to polymersomes [11–13] and it has been recently shown that the hybrid vesicles permeability could be increased by

adding phospholipase A2 that can selectively degrade lipids [14]. Examples of hybrid nanoscale polymersomes have been proposed for applications in nanomedicine and seemed to improve the targeting efficiency [15,16]. Interestingly, hybrid vesicles at the micron scale are valid alternatives to giant liposomes as simplified cell models for a deeper understanding of fundamental biological processes [17,18]. They have indeed the potential for mimicking the membrane functionalities like the presence of raft-like domains [19,20], membrane asymmetry [21] transport or recognition properties thanks to the insertion of proteins in the membrane [22–24] and even chemical energy-driven ATP production [25] or cell compartmentalization [26]. To date, the potential responsiveness of block copolymers has not yet been exploited for hybrid vesicles. Indeed, only examples of temperature-responsive hybrid vesicles are reported in the literature, exploiting the phase transition of dioleylphosphatidyl choline based lipids [27].

One of the reasons of the lack of polymer/lipid hybrid systems is the limited choice of the amphiphilic copolymers which were generally restricted to a small group based on the combination of poly(ethylene oxide) or poly(oxazoline) as hydrophilic unit and either poly(dimethyl siloxane) (PDMS) [28,29], poly(butadiene) (PBD) [30,31], polyisobutylene (PIB) [32] and very recently butylacrilate [33] as hydrophobic moiety.

Different methodologies have been used to form polymer based giant unilamellar vesicles (GUVs). They have been mainly inspired from those developed for lipids [34]. Electroformation method is the most employed one. It is a solvent-free method where a dry amphiphilic thin film is hydrated in the presence of an alternating current probably inducing fluctuations and interlayer repulsions, which favours the swelling and release of giant vesicles [35]. It was applied to block-copolymers for the first time in the case of poly(ethylene oxide)-*block*-poly(ethyl ethylene) [36]. Electroformation can be applied to a limited class of block-copolymers [33,37,38], as the choice

of the nature of the block copolymer is usually dictated by the hydrophobic block glass transition temperature, since this should be as low as possible in order to guarantee a sufficient flexibility and mobility of the polymer chains. Gentle hydration has been described even earlier than electroformation for brain phospholipids [39] and is quite difficult to be applied to block-copolymers as witnessed by the very limited number of publications [40–42]. Gel assisted hydration using polyvinyl alcohol (PVA) [43] or agarose [44] have been proposed for lipid vesicles and PVA was also used for polymer-based vesicles [45]. In this case, the presence of unwanted impurities in the bilayer or lumen cannot be excluded.

Emulsion phase (or droplet) transfer has been developed for lipids [46], improved in microfluidic devices [47,48] or special centrifugation set-ups [49–51] (continuous droplet interface crossing encapsulation, i.e. cDICE) and has been rarely used for block copolymers [21,52]. This method is based on a water-in-oil emulsion where water droplets are coated with the amphiphilic species. These droplets are allowed to cross the interface of an oil-on-water biphasic system stabilized by an amphiphilic monolayer, thus forming the vesicles. A known drawback of this method is the presence of residual oil between the lipid leaflets [53]. However, membrane bending rigidity analysis revealed that mineral oil doesn’t affect the mechanical properties of the membrane [54].

Because hybrid GUVs are essential tools for developing synthetic reactors or biomimetic cells and are so far very limited, in this work we propose to use block copolymers based on methylmethacrylate (MMA) and N,N-dimethylaminoethyl methacrylate (DMAEMA) mixed with palmitoyl oleyl phosphatidyl choline (POPC) in order to obtain giant hybrid vesicles. The presence of pH-sensitive DMAEMA unit could provide the access to systems with pH-responsive permeability. In the literature MMA/DMAEMA based block-copolymers have been

mainly used to develop nano-sized polymersomes. Polymeric nano-vesicles based on butyl-methacrylate (BMA) and DMAEMA were developed as reactors for the urea-urease system, for example [55]. We recently showed that the copolymer poly(ethylene glycol monomethyl ether)-*block*- poly(methyl methacrylate –*random*- N,N-dimethyl amino ethyl methacrylate), mPEG-*block*-P(MMA-*ran*-DMAEMA), was able to form nano-vesicles in a wide range of DMAEMA chemical compositions and architectures (linear and branched) [56]. Furthermore, they exhibited a pH-dependent swelling characterized by a strong increase in size, up to 10 times passing from pH 7.4 to pH 4.4. This swelling was attributed to electrostatic repulsions at low pH, linked to the concurrent increase of protonated DMAEMA units.

As for giant vesicles, which were not necessarily unilamellar ones, poly(methacrylic acid)-*block*-poly(methylmethacrylate-*random*-methacrylic acid), PMAA-*block*-P(MMA-*ran*-MAA) could form giant vesicles in a photo-polymerization induced self-assembly process in an aqueous methanol solution [57,58]. The authors investigated the pH-responsive behaviour of the vesicles showing that they were disrupted in basic environment (pH 12) and they could be reversibly reconstructed at neutral pH. Yoshida also characterized polymeric giant vesicles with copolymers containing DMAEMA units inserted in the P(MMA-*ran*-MAA) block [59]. These vesicles were unstable and had many holes on the surface. When quaternized DMAEMA was used the vesicles were stable, but they had much smaller size (below 1 μm).

Hybrid GUVs made of poly(cholesteryl methacrylate)-*block*-poly(2-(dimethylaminoethyl methacrylate) (pCMA-*block*-pDMAEMA) were characterized with confocal microscopy by W. Zong et al. [16] to confirm the presence of both phospholipids and the block copolymer in the same membrane, pCMA constitutes the hydrophobic block, while the pH-sensitive pDMAEMA constitutes the hydrophilic block. These GUVs were electroformed and the maximum polymer

content was 70% w/w (corresponding to 3.6 mol % using Mn=47.5 kD as reported in Table 1 of the cited work). Also, hybrid nano-vesicles were formed by this copolymer mixed with phospholipids containing palmitoyl and oleyl as fatty acyl groups and different charged headgroups (i.e. phosphatidylcholine, ethylphosphocholine and phosphatidylserine) showed a prevalent cytosolic localization when incubated with mouse macrophages, indicating a good potential for applications in drug delivery [16].

In this paper, we want to show that a block copolymer with high molecular weight and high T_g can be successfully incorporated into hybrid giant vesicles. We propose to use mPEG-*block*-P(MMA-*grad*-DMAEMA) in combination with 1-palmitoyl-2-oleoyl-*sn*-glycero-3-phosphocholine (POPC) to prepare vesicles by means of two formation methods, namely electroformation and droplet transfer; it will be shown that the high T_g polymer diminishes the efficiency of the electroformation method even at low (~ 15 mol %) polymer content, whilst the droplet transfer method allows the formation of hybrid vesicles for a wide range of polymer/lipid ratios. With this approach, the polymer content in the hybrid GUVs has been sensibly increased with respect to that already reported in the literature (~ 4 mol %).

2. MATERIALS AND METHODS

Materials

Copper bromide ($CuBr_2$), 2,2'–bipyridine (bpy), tin (II) 2-ethylhexanoate ($Sn(EH)_2$), 2,4-dimethyl-3-ethylpyrrole, trifluoroacetic acid (TFA), dichlorodicyanoquinone (DDQ), triethylamine (Et_3N), boron trifluoride etherate ($BF_3{\cdot}Et_2O$), butylated hydroxytoluene (BHT), basic alumina, Sephadex LH-20, 1-palmitoyl-2-oleoyl-*sn*-glycero-3-phosphocholine, Mineral oil M5904, toluene, methanol, dimethylformamide (DMF), n-hexane, poly(ethylene glycol)

monomethylether (mPEG, M_n = 2000 $gmol^{-1}$, M_w/M_n = 1.16 and M_n = 5000 $gmol^{-1}$, M_w/M_n = 1.02) and pyranine were purchased from Sigma-Aldrich and used without further purification. 18:1 Liss Rhodamine PE was used as received by Avanti Polar Lipids. Methylmethacrylate (MMA) and N,N-(dimethylamino)ethylmethacrylate (DMAEMA) (Sigma-Aldrich) were purified prior copolymerizations by means of a column filled with basic alumina to remove the inhibitors. Dichloromethane (Sigma-Aldrich) used for BODIPY synthesis was distilled over $CaCl_2$.

All manipulations involving air-sensitive compounds were carried out under nitrogen atmosphere using Schlenk techniques.

Synthesis of the fluorescent-labeled DMAEMA monomer 2,6-diethyl-1,3,5,7-tetramethyl-8-[4-[8-(2-methacryloylethyl)dimethylammoniumbromideoctyloxy]phenyl]-4,4'-difluoroboradiaza indacene (BODIPY-DMAEMA)

As a first step, the precursor 2,6-diethyl-1,3,5,7-tetramethyl-8-[4-(8-bromooctyloxy)phenyl]-4,4'-difluoroboradiaza indacene was synthesized. 4-(8-bromooctyloxy)benzaldehyde was prepared as previously described [60]. 720 µL of 4-(8-bromooctyloxy)benzaldehyde (2.3 mmol) and 756 µL of 2,4-dimethyl-3-ethylpyrrole (5.6 mmol) were then dissolved in 50 mL of absolute CH_2Cl_2 under N_2 atmosphere, ten drops from a Pasteur pipette of TFA were added and the solution was stirred at RT overnight or until TLC analysis showed complete consumption of the aldehyde. At this time, 785 mg of DDQ (3.45 mmol) were added and stirring continued for 20 min. Then, 5 mL of Et_3N and 5 mL of $BF_3{\cdot}OEt_2$ were added. The mixture was stirred for 12 h and the organic layer containing the crude product was subsequently washed three times with water; the organic solution was dried over Na_2SO_4, and evaporated to dryness. The raw material was purified by chromatography (SiO_2, petroleum ether - CH_2Cl_2, 1:1) to afford 246 mg of product (yield: 18.2%)

in the form of orange needles. $C_{31}H_{42}BBrF_2N_2O$, MM = 587.39 $gmol^{-1}$, UV-vis (CH_2Cl_2): 528 nm (ε = 92600 M^{-1} cm^{-1}). Quantum efficiency of fluorescence Φ_{fluo} (in CH_2Cl_2): 0.45 (544 nm) was calculated according to the following equation:

$$\Phi_{fluo}{}^{sample}=\Phi_{fluo}{}^{standard}\times(I_{fluo}{}^{sample}/I_{fluo}{}^{standard})\times(Abs^{standard}/Abs^{sample})$$

where I_{fluo} is the fluorescence intensity at the specific excitation wavelength, Abs denotes the absorbance at the excitation wavelength.

^1H NMR ($CDCl_3$) δ: 1.00 (t, 6H, 2×CH_3); 1.46 (s, 6H, 2×CH_3); 1.45-1.55 (m, 8H, 4×CH_2); 1.82-1.93 (m, 4H, 2×CH_2); 2.32 (q, 4H, 2×CH_2); 2.58 (s, 6H, 2×CH_3); 3.45 (t, 2H, CH_2Br); 4.03 (t, 2H, CH_2O); 6.00 (s, 2H, 2×CH); 7.02 (d, 2H, 2×CH); 7.18 (d, 2H, 2×CH).

To obtain the fluorescent-labeled DMAEMA monomer, 10 mg (0.045 mmol) of 2,6-diterbutyl-4-methylphenol (BHT) were added to a mixture of 236 mg of 2,6-diethyl-1,3,5,7-tetramethyl-8-[4-(8-bromooctyloxy)phenyl]-4,4'-difluoroboradiaza indacene (0.402 mmol) in 3 mL of DMAEMA (17.75 mmol), reaction scheme and chemical structures are reported in Figure S1 of the supporting information. The mixture was kept at 70 °C for 24 h. During the reaction time, a solid product was formed. After filtration, the product was washed 4 times with 20 mL of diethyl ether affording 214 mg (71.4%) of product. $C_{39}H_{57}BBrF_2N_3O_3$, MM = 744.60 $gmol^{-1}$ (ESI-MS spectrum is reported in Figure S2 of the supporting information). ^1H NMR ($CDCl_3$) δ: 0.97 (t, 6H, 2×CH_3); 1.33 (s, 6H, 2×CH_3); 1.40 (m, 8H, 4×CH_2); 1.80 (m, 4H, 2×CH_2); 1.95 (s, 3H, CH_3), 2.25-2.33 (q, 4H, 2×CH_2); 2.51 (s, 6H, 2×CH_3); 3.56 (s, 6H, 2×CH_3); 3.61-3.65 (t, 2H, CH_2); 3.97-4.02 (t, 2H, CH_2); 4.15 (t, 2H, CH_2); 4.65 (t, 2H, CH_2); 5.68 (s, 1H, CH); 6.15 (s, 1H, CH); 6.96-6.99 (d, 2H, 2×CH); 7.13-7.15 (d, 2H, 2×CH). Details of ^1H peak assignment and HSQC-NMR spectra are reported in Figures S3 – S5 of the supporting information.

Synthesis of mPEG-block-P(MMA-grad-DMAEMA) copolymers.

Macroinitiator mPEG-Br was synthesized according to the procedure reported in literature. [61] In a typical procedure, the copolymerization of MMA/DMAEMA was carried out in a 50 mL glass flask charged, under nitrogen atmosphere, with 0.1 g of mPEG-Br macroinitiator in 5 mL of toluene. Subsequently, 100 μL of $CuBr_2$ (1×10^{-3} M in DMF, 10^{-4} mmol), 100 μL of bpy (1×10^{-2} M in DMF, 10^{-3} mmol), 100 μL of $Sn(EH)_2$ (1×10^{-2} M in toluene, 10^{-3} mmol), 2-4 mL of MMA (18.8-37.6- mmol) and 1.2 – 2.5 mL of DMAEMA (7.10 – 14.8 mmol) were added (the volumes of MMA and DMAEMA were varied to change the final composition in the copolymer). The mixture was thermostated at 60 °C and magnetically stirred. The reaction was stopped after 4h by adding *n*-hexane. The copolymer was recovered by filtration, washed with cold methanol (~ 4 °C) and dried in vacuum at 40 °C. ^{1}H-NMR (400 MHz, $CDCl_3$): δ 0.87-1.03 (-C*H*$_3$ main chain), 1.83-1.91 (-C*H*$_2$- main chain), 2.30 (-N(C*H*$_3$)$_2$)), 2.58 (–OCH$_2$ C*H*$_2$ N(CH$_3$)$_2$), 3.61 (-OC*H*$_3$), 3.66 (-OC*H*$_2$C*H*$_2$-), 4.08 (-OC*H*$_2$ CH$_2$ N(CH$_3$)$_2$). ^{13}C-NMR(400 MHz, $CDCl_3$): δ 16.9-19.1 (-*C*H$_3$ main chain), 44.9-45.3 (quaternary carbon in the main chain), 46.2 (-N(*C*H$_3$)$_2$), 52.2 (-O*C*H$_3$, MMA), 54.6 (-*C*H$_2$- main chain), 57.6 (-OCH$_2$ *C*H$_2$ N(CH$_3$)$_2$), 63.5 (-O*C*H$_2$ CH$_2$ N(CH$_3$)$_2$), 70.9 (-O*C*H$_2$ *C*H$_2$-), 176.3-178.2 (-C=O). Details of ^{1}H peak assignment and ^{13}C NMR spectra are reported in Figure S6 of the supporting information.

Chemical composition and the molecular weight (M_n) were evaluated via ^{13}C NMR. The molar fractions of the components in the final copolymers were evaluated through the equations:

$$X_{\mathrm{mPEG}} = \frac{I_{\mathrm{mPEG}}}{I_{\mathrm{mPEG}} + 2I_{\mathrm{MMA}} + I_{\mathrm{DMAEMA}}} \quad (1)$$

$$X_{\mathrm{MMA}} = \frac{2I_{\mathrm{MMA}}}{I_{\mathrm{mPEG}} + 2I_{\mathrm{MMA}} + I_{\mathrm{DMAEMA}}} \quad (2)$$

$$X_{\mathrm{DMAEMA}} = \frac{I_{\mathrm{DMAEMA}}}{I_{\mathrm{mPEG}} + 2I_{\mathrm{MMA}} + I_{\mathrm{DMAEMA}}} \quad (3)$$

where I_{mPEG} is the integration of the signal relative to mPEG units: $-OCH_2CH_2-$, I_{MMA} is the signal corresponding to the units $-OCH_3$ of MMA and I_{DMAEMA} integrates the two carbons of the amine group of DMAEMA ($-N(CH_3)_2$). M_n was calculated from the following equation:

$$M_n = DP_{\mathrm{mPEG}} MM(\mathrm{EO}) + DP_{\mathrm{MMA}} MM(\mathrm{MMA}) + DP_{\mathrm{DMAEMA}} MM(\mathrm{DMAEMA}) \quad (4)$$

where:

$DP_{\mathrm{mPEG}} = M_{\mathrm{nPEG}}/44$

$DP_{\mathrm{MMA}} = DP_{\mathrm{mPEG}} (2I_{\mathrm{MMA}}/I_{\mathrm{mPEG}})$

$DP_{\mathrm{DMAEMA}} = DP_{\mathrm{mPEG}} (I_{\mathrm{DMAEMA}}/I_{\mathrm{mPEG}})$

The synthesis of the fluorescent-labelled copolymer was carried out under the same experimental conditions described above by adding 2 mL of MMA (18.8 mmol), 1.2 mL of DMAEMA (7.10 mmol), 2 mL of DMF and 5 mg of the fluorescent monomer BODIPY-DMAEMA (6.7×10^{-3} mmol) to the reaction mixture. The applied procedure of purification [62,63] was based on the use of lipophilic Sephadex LH-20 to separate molecules with different molecular weights. A mini column (Pasteur pipette) was loaded with the lipophilic stationary phase (~1.5 g of Sephadex previously swollen for one hour in 10 mL of methanol) and filled with methanol to elute the samples. ^{1}H-NMR (400 MHz, $CDCl_3$): δ 0.87-1.04 ($-CH_3$ main chain), 1.27 ppm (6 CH_2 of the alkyl chain of the BODIPY-DMAEMA), 1.83-1.91 ($-CH_2-$ main chain), 2.30 ($-N(CH_3)_2$)), 2.59 ($-OCH_2$ CH_2 $N(CH_3)_2$), 3.61 ($-OCH_3$), 3.65 ($-OCH_2CH_2-$), 4.08 ($-OCH_2$ CH_2 $N(CH_3)_2$). ^{13}C-NMR (400 MHz, $CDCl_3$): δ 16.5-18.7 ($-CH_3$ main chain), 29.7 ppm (6 CH_2 of the

alkyl chain of the BODIPYDMAEMA), 44.6-44.9 (quaternary carbon in the main chain), 45.8 (-N(CH_3)$_2$), 51.8 (-OCH_3, MMA), 54.4 (-CH_2- main chain), 57.2 (-OCH$_2$ CH_2 N(CH_3)$_2$), 63.1 (-OCH_2CH_2 N(CH_3)$_2$), 70.6 (-OCH_2CH_2-), 176.3-178.2 (-C=O). Details of ^{1}H peak assignment, ^{13}C NMR and HSQC-NMR spectra are reported in Figures S7 and S8 of the supporting information.

Chemical composition and the molecular weight (M_n) were evaluated via ^{13}C NMR through the equations:

$$X_{\mathrm{mPEG}} = \frac{I_{\mathrm{mPEG}}}{I_{\mathrm{mPEG}} + 2I_{\mathrm{MMA}} + I_{\mathrm{DMAEMA}} + \frac{I_{\mathrm{BODIPYDMAEMA}}}{2}} \quad (5)$$

$$X_{\mathrm{MMA}} = \frac{2I_{\mathrm{MMA}}}{I_{\mathrm{mPEG}} + 2I_{\mathrm{MMA}} + I_{\mathrm{DMAEMA}} + \frac{I_{\mathrm{BODIPYDMAEMA}}}{2}} \quad (6)$$

$$X_{\mathrm{DMAEMA}} = \frac{I_{\mathrm{DMAEMA}}}{I_{\mathrm{mPEG}} + 2I_{\mathrm{MMA}} + I_{\mathrm{DMAEMA}} + \frac{I_{\mathrm{BODIPYDMAEMA}}}{2}} \quad (7)$$

$$X_{\mathrm{BODIPYDMAEMA}} = \frac{\frac{I_{\mathrm{BODIPYDMAEMA}}}{2}}{I_{\mathrm{mPEG}} + 2I_{\mathrm{MMA}} + I_{\mathrm{DMAEMA}} + \frac{I_{\mathrm{BODIPYDMAEMA}}}{2}} \quad (8)$$

where I_{mPEG} is the integration of the signal relative to mPEG units: -OCH$_2$CH$_2$-; I_{MMA} is the integration of the signal relative to MMA units: -OCH$_3$; I_{DMAEMA} is the integration of methyl group of the signal relative to DMAEMA units; $I_{\mathrm{BODIPYDMAEMA}}$ are the 4 CH_2 of the fluorescent mojety (signals labeled $i_{1\text{-}4}$ in the NMR spectra, figures S7-S8 of the supporting info). The

degrees of polymerization and hence the molecular weights were calculated from the following equation:

$$M_n = DP_{mPEG}(MM_{EO}) + DP_{MMA}(MM_{MMA}) + \\ + DP_{DMAEMA}(MM_{DMAEMA}) + DP_{BODIPYDMAEMA}(MM_{BODIPYDMAEMA}) \quad (9)$$

where:

$$DP_{mPEG} = M_{n(mPEG)}/44$$
$$DP_{MMA} = DP_{mPEG}\left(2I_{MMA}/I_{mPEG}\right)$$
$$DP_{DMAEMA} = DP_{mPEG}\left(I_{DMAEMA}/I_{mPEG}\right)$$
$$DP_{BODIPYDMAEMA} = DP_{mPEG}\left(I_{BODIPYDMAEMA}/2I_{mPEG}\right)$$

NMR Analysis.

^{1}H and ^{13}C NMR spectra were recorded at 25 °C in $CDCl_3$ using a Bruker Avance 400 MHz spectrometer (D1 = 5 s for ^{13}C NMR). Samples were prepared by introducing 20 mg of copolymer and 0.5 mL of $CDCl_3$ into a tube (5 mm outer diameter). Chemical shifts (δ) are listed as parts per million: ^{1}H NMR spectra are referenced using the residual solvent peak at δ = 7.26 ppm, in ^{13}C NMR spectra the residual solvent peak is at δ = 77.2 ppm.

DSC.

*T*he glass transition temperatures were measured with Dynamic Scanning Calorimetry (Mettler Toledo DSC1 STAR SYSTEM FRS5). About 10 mg of sample were inserted in a 100 μL aluminum pan and heating/cooling cycles were registered at 20 K/min. In the first run, the

sample was heated from 25 °C to 165 °C, followed by cooling to -60 °C. In the other two runs, the sample was heated from -60 °C to 165 °C and cooled from 165 °C to -60 °C. The T_g was measured on the second heating run where the inflection point is generally more evident.

Microscopy.

Images were acquired on an inverted optical microscope (Eurotek Orma INV100TFL) using a 20× objective and then analysed with the software ImageJ. The mixed membranes were characterized with a confocal microscope (Leica TCS SP2 and TIRF OLYMPUS FV1000). The fluorescent polymer and the fluorescent lipid were excited respectively at 488 nm, with an Ar laser, and at 561 nm, with a DPSS 561 laser and the fluorescence was collected with photomultipliers tubes PMTs in the wavelength ranges 498 – 530 nm and 571 – 630 nm, respectively.

Preparation of Giant Vesicles.

Droplet Transfer Method. Stock solutions of [POPC] = 3 mM (2.28 mg mL^{-1}) and [copolymer] = 5 mg mL^{-1} (0.36 mM by using the copolymer average molecular weight M_n = 13850 g mol^{-1}) were prepared in mineral oil. The fluorescent probes, being less soluble in mineral oil, were dissolved in $CHCl_3$ at the concentration $[\text{fluo-polymer}]_{CHCl3}$ = 10 mg mL^{-1} (0.027 mM using an average molecular weight M_n = 370928 g mol^{-1}) and $[\text{18:1 Liss Rhod PE}]_{CHCl3}$ = 0.77 mM (1 mg mL^{-1}). Giant Unilamellar vesicles were prepared with the Droplet Transfer Method described by Pautot et al. for lipid-based GUVs [46] using lipid:copolymer molar ratios 93:7, 85:15 and 60:40 (corresponding to lipid:copolymer weight ratios 0.42:0.58, 0.24:0.76, 0.08: 0.92 by using the copolymer average molecular weight M_n = 13850 g mol^{-1}). An Eppendorf tube was filled with 500 μL of an aqueous phase containing 200 mM of glucose (O-solution), then 300 μL of a

hydrophobic interfacial phase containing lipids and polymers at various ratios (obtained by mixing the POPC and polymer stock solution) was poured on top of the O-solution. A second Eppendorf tube was used to prepare a water/oil microemulsion: 20 μL of an aqueous solution containing 200 mM of sucrose (inner solution, I-solution), were mixed by pipetting with 600 μL of an oil phase containing the same amount of lipids and polymers as the interfacial phase and 5 μL of chloroform solutions of fluorescent probes (chloroform was firstly evaporated in argon stream ~~before~~ and then oil containing other amphiphiles was added). The microemulsion was then poured over the interfacial phase and vesicles were formed by centrifuging the tube at 6000 rpm for 10 minutes at room temperature. Vesicles were collected as a pellet at the bottom of the aqueous phase and gently washed with 100 μL of O-solution and finally observed at the microscope. In these experimental conditions, however, pure polymeric vesicles could not be formed. When POPC was not present in the initial oil solution, the precipitation of a drop of coloured polymer (i.e. containing the fluorescent polymeric probe or pyranine when employed) was always detected at the bottom of the Eppendorf tube. Problems might be related with difference in density between the I- and O-solution that could be overcame by employing a different nonpolar solvent or by changing the concentrations of the sugars.

Electroformation. GUVs were prepared on a *Vesicles prep pro* instrument produced by Nanion through the electroformation method described by *Angelova et al.* [64] for lipid-based giant vesicles. Stock solution of [POPC] = 1.32 mM (1 mg mL^{-1}) and [copolymer] = 1 mg mL^{-1} (0.072 mM if we consider a copolymer average weight of 13850 g/mol) and POPC where prepared at 1 mg mL^{-1} (both polymer and lipid) in chloroform and [copolymer] = 1 mg mL^{-1} (0.072 mM by using the copolymer average molecular weight M_n = 13850 g mol^{-1}). For electroformation, they were mixed in different ratios so that the total final concentration of the polymer plus POPC was

0.25 mg mL^{-1} and the total deposited amount was fixed in order to avoid the formation of a thick film. The POPC concentration was 0.136 mM, 0.08 mM and 0.05 mM in the samples with POPC:copolymer molar ratios equal to 93:7, 85:15 and 70:30 respectively (corresponding to lipid:copolymer weight ratios 0.42:0.58, 0.24: 0.76, 0.11: 0.89 by using the copolymer average molecular weight M_n = 13850 g mol^{-1}).

5 μL of the obtained chloroform solutions of the polymer and lipid at different molar ratios were spread onto ITO-coated glass slide and dried under vacuum for at least 3 hours. The dry film was surrounded with a 1 mm O-ring in order to delimit the electroformation chamber which was subsequently filled with 250 μL of a 240 mM sucrose solution. Another ITO-coated glass slide was used to close the chamber, which was further connected to an alternate voltage generator. A peak-to-peak voltage of 3 V and a frequency of 10 Hz were applied at 65 °C for at least 2 hours to form the GUVs. The temperature and the voltage were then slowly decreased and the vesicles were collected with a pipette.

3. RESULTS AND DISCUSSION

A mandatory condition that has to be satisfied to control the formation, the stability and the characteristics of mixed polymer/lipid vesicles is the similarity of the solubility parameter (δ) [65,66] of the phospholipids' fatty acids chains with the hydrophobic part of the amphiphilic synthetic copolymer. In this respect, the comparable values of PMMA (δ = 18.7 $MPa^{1/2}$ [67]) with that of the fatty acid chains (δ = 18.2 $MPa^{1/2}$ [20]), allows us to consider as good the compatibility between an amphiphilic block copolymer containing PMMA and the phospholipid chosen for the formation of the hybrid vesicles (POPC).

However, a rational design in terms of molecular weight, composition and hydrophilic/hydrophobic ratio is also needed since one of the main issue for the formation of hybrid vesicles also includes the similitude or the discrepancy of the size of the hydrophobic segments in the copolymers and phospholipids, other than a proper glass transition temperature (T_g) of the synthetic copolymer [20].

To this end, several MMA-based block copolymers having different properties (M_n, Hydrophilic-Lipophilic Balance HLB, etc.) were synthesized by a modified version of the ATRP, namely the Activators ReGenerated by Electron Transfer ATRP (ARGET-ATRP) [68,69].

The copolymers have a linear, A-*block*-(BC), architecture and consist of a hydrophilic block (A) based on poly(ethylene glycol) monomethylether (mPEG), and a hydrophobic block (BC) made of a copolymer chain containing methyl methacrylate (MMA, B) and N,N-(dimethylamino)ethyl methacrylate (DMAEMA, C) as represented in Figure 1.

The DMAEMA monomer was introduced both to modulate the PMMA T_g, and to give potential pH-sensitivity for further applications to the hybrid vesicles [56,70–72]. However, though the chain based on MMA/DMAEMA has an increasing hydrophilicity with decreasing pH, at pHs ranging from neutrality to basic conditions, the hydrophobicity, and consequently the δ value, remains compatible with the POPC fatty acid chain.

Copolymers were thus synthesized using mPEG-Br (M_n = 2000 g mol^{-1} and M_n = 5000 g mol^{-1}) as macroinitiator in presence of $CuBr_2$/bpy and $Sn(EH)_2$ as reducing agent in toluene at 60 °C (Figure 1). The experimental conditions, meaning relative amount of MMA and DMAEMA in

the feed, were systematically changed in order to find the most suitable microstructure for the formation of mixed vesicles with POPC.

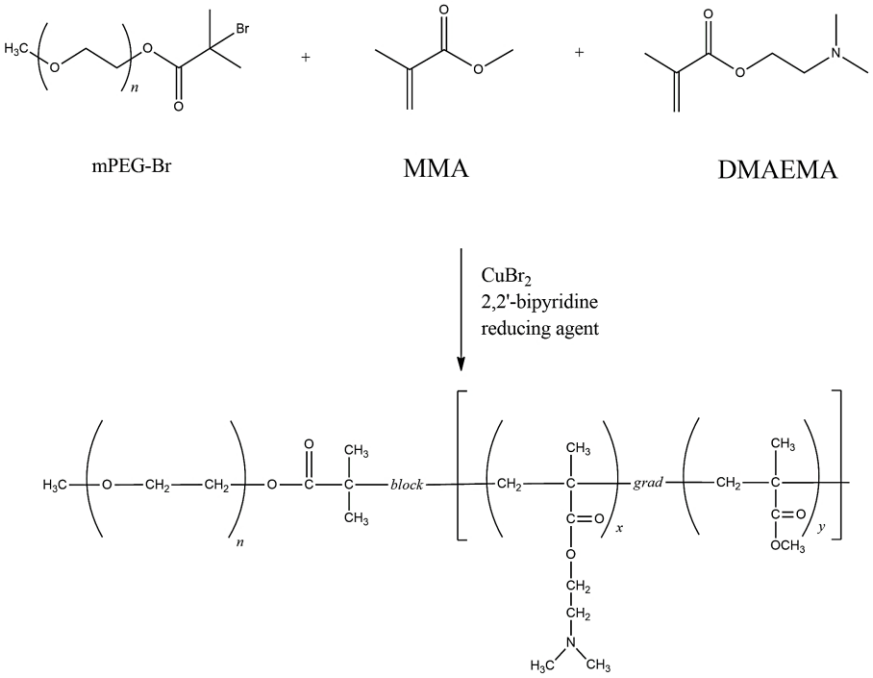

Figure 1. Reaction scheme for the synthesis of mPEG-*block*-P(MMA-*grad*-DMAEMA) copolymers

The large difference in the reactivity ratios found between MMA and DMAEMA suggested that the "BC" block is characterized by a *gradient-like* composition with the initial part of the chain (i.e. the one closer to the mPEG block) richer in the monomer DMAEMA, that smoothly changes towards a prevalent MMA composition [73]. This microstructure in principle could favour the formation of blended vesicles allowing the insertion of the hydrophobic moiety of the copolymer within the phospholipid carbon chains. The characteristics of all copolymers synthesized are reported in Table 1.

Table 1. Chemical composition, molar masses, HLB and T_g of the copolymers synthesized

Sample	M_n mPEG	X_{mPEG} (mol)	X_{MMA} (mol)	X_{DMAEMA} (mol)	M_n[a] (kg mol^{-1})	HLB[b]	T_g[c] (°C)

1	2000	0.24	0.76	---	16.3	2.45	97
2	5000	0.14	0.51	0.35	62	1.61	85
3	5000	0.44	0.35	0.21	23	4.35	50
4	5000	0.50	0.27	0.23	19.4	5.15	55
5	2000	0.34	0.26	0.40	13.8	2.90	44

[a] Determined by ^{13}C-NMR using equation (4)

[b] Calculated by Griffin method: HLB = 20(M_h/M) where M_h is the molar mass of the hydrophilic portion (mPEG) and M is the molar mass of the copolymer

[c] heating rate 20 K/min

Considering that the T_g of the homopolymers is ~ - 65 °C for PEG, ~ 105 °C for PMMA and ~ 20 °C for PDMAEMA, data reported in Table 1 show that the lower is the content of MMA and the value of molecular weight (e.g. samples 3 – 5), the lower is the T_g of the corresponding copolymer. Among the copolymers in Table 1, we selected the one with a molar composition of 34% – 26% – 40% of mPEG – MMA – DMAEMA, respectively and M_n = 13.8 kg mol^{-1} (sample 5) to produce hybrid GUVs using the electroformation method. This copolymer has the lowest T_g and average molecular weight together with a HLB (hydrophilic-lipophilic balance) value similar to the one of POPC (3.98), it then appears the most suitable for the preparation of hybrid vesicles. It is reasonable that the HLB value together with a low steric mismatch between copolymers and POPC molecular weight should ensure a major compatibility with the lipid. Besides, as it has the lowest T_g value is the best candidate for electroformation where the higher the polymer chain mobility the higher the yield of vesicle formation.

Giant vesicles, containing different percentages of lipid and copolymer were produced by using two different processes: an electroformation and a phase transfer method.

As copolymer 5 did not form pure GUVs by electroformation, we decided to explore compositions with high molar amount of POPC. A large number of electroformed POPC giant

vesicles could be easily obtained within 30 minutes at room temperature, as reported in Figure S9 a) of the Supporting Information. Even a small amount of copolymer (< 5 mol%) added to POPC inhibited the vesicle formation at 25 °C and the temperature had to be increased till 65 °C in order to be able to obtain a few vesicles after 2 hours, as shown in Figure S9 b) in the Supporting Information. The maximum initial copolymer content clearly allowing vesicles formation was 15 mol%, though the typical microscopy images showed few electroformed aggregated vesicles (often containing solid residues of presumably precipitated polymers and/or lipids), which hardly detached from the film. In the presence of higher initial percentage of polymer, only scant irregular objects could be detected.

These results clearly show that the presence of the polymer, even at low percentage (< 15 mol%), with a high glass transition temperature hinders POPC vesicles electroformation. For this reason we decided to use the phase transfer method, developed for giant liposomes and previously employed for the synthesis of asymmetric hybrid polymer-lipid giant vesicles [21]. With this method, the same amount of copolymer and lipid was dispersed in both the interfacial phase and in the emulsion in order to favour a symmetric composition of the two leaflets of the bilayer. In order to get insight into the nature of the formed vesicles, two fluorescent probes were employed to highlight the possible partitioning of the two different components, lipid and copolymer, within the hybrid GUVs. A fluorescent lipid, 18:1 Liss Rhod PE, known for its affinity for the liquid disordered domains in phase separated model membranes [74] and also used as a marker for the lipid-rich region in hybrid vesicles [75–78], was chosen. To stain the polymer-rich domains, a modified DMAEMA with a pendant group consisting of a BODIPY-based fluorescent dye was synthesized and used to obtain a labeled mPEG-*block*-P(MMA-*grad*-DMAEMA) copolymer (composition:, mPEG = 4.4%, MMA = 51%, DMAEMA = 38%,

BODIPY = 6.2%, indicated as BODIPY-copolymer). The chemical structure of this BODIPY-copolymer should guarantee a preferential partition of the probe in the polymer-rich region. The affinity between the BODIPY-copolymer probe and the copolymer 5 has been checked by DSC measurements (Figure S10 in the Supporting Information). The presence of a single T_g transition, different from the ones of neat copolymers, clearly indicates that they are molecularly miscible. On the other hand, blends of the BODIPY-copolymer and POPC did not show changes in phase transitions (Figure S11 in the Supporting Information).

Because of the difficulties related to the phase transfer method in determining the final composition of vesicles [79–81], the percentages of lipids and polymers reported hereon refer to the initial amount of the components in the solutions prior the centrifugation phase. In a first step, lipid vesicles stained with the fluorescent dye were prepared at pH ~ 7 to characterize the absorption and emission spectra useful for the observation at the confocal microscope. Figure 2 a) and b) show confocal images, respectively, at the characteristic emission wavelengths for the fluorescence of BODIPY ($498 < \lambda < 530$ nm) and for 18:1 Liss Rhod PE ($571 < \lambda < 630$ nm), when blended in the double layer of POPC vesicles. Figure 2 a) clearly shows that a very low amount of the BODIPY-copolymer = 0.02 mol% with respect to the total amount of amphiphiles, can be homogenously dispersed into the POPC phospholipid membranes and confirms that the solubility parameter of the synthesized copolymer is close to that of pure PMMA.

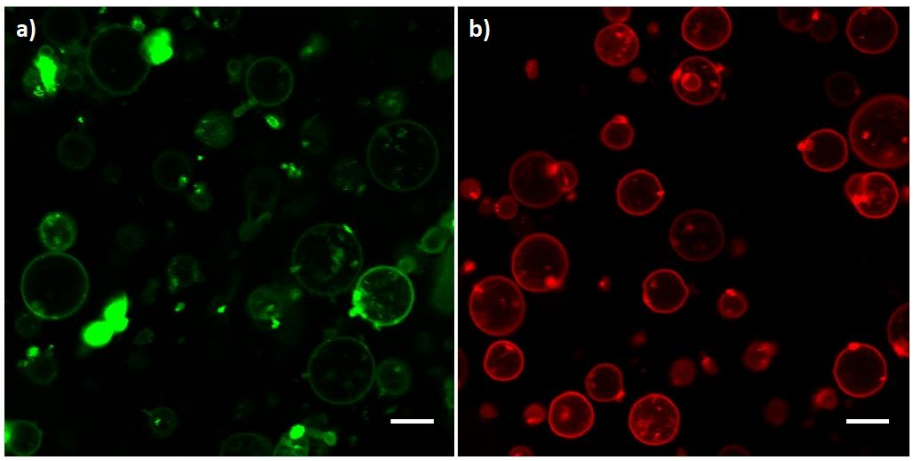

Figure 2 POPC vesicles labelled with fluorescent probes. a) POPC and BODIPY-copolymer 99.98 %: 0.02 %; b) POPC and 18:1 Liss Rhod PE 99 %: 0.8%. Small round spots in a) and b) are probably due to mineral oil residues. White bar scales 10 µm.

Mixed vesicles were successfully prepared at pH = 7, where 50% of the copolymer is protonated (pKa ~ 7, see Figure S12 in Supporting Information), by varying the unlabeled copolymer mole percentage in the range 8 – 40 % (58 – 89 wt%), higher concentration of copolymer hindered the self-assembly of the amphiphiles and the formation of a pellet at the end of the phase transfer procedure was not obtained. Furthermore, we could not observe the formation of pure polymer GUVs.

Vesicles with the compositions mol % POPC – mol % copolymer 5: 92% – 8%, 85% – 15%, 60% – 40% labeled with 18:1 Liss Rhod PE and BODIPY-copolymer are shown in Figure 3 a) – c), respectively. In each figure, the green channel represents the fluorescence of the copolymer, the red channel corresponds to the fluorescence of the lipid and the yellow channel represents their overlap. When the concentration of the copolymer in the vesicles was below ~20 mol% the mixed membranes were mainly heterogeneous, with small regions where copolymer blended into the lipid layers. Interestingly, the presence of the copolymer in the membranes promoted the

fusion of single vesicles into budded structures, as shown in Figure 3 a), or large aggregates of fused vesicles. The welding surface between vesicles was indeed characterized by a large concentration of copolymer, highlighted by the intense yellow colour, which probably favours electrostatic interaction between the outer leaflets of the membranes, as previously observed in the presence of charged fatty acids incorporated in the double layer of POPC vesicles [82,83].

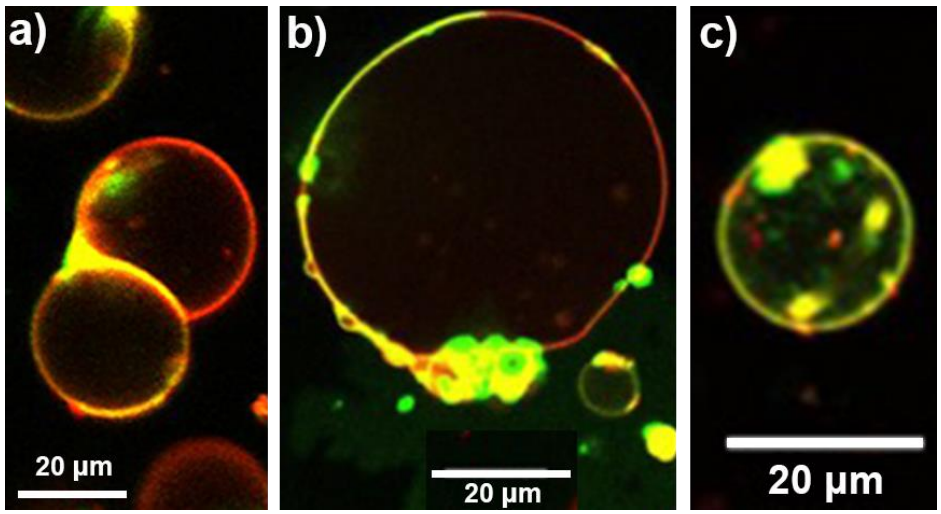

Figure 3 Mixed POPC- copolymer vesicles having molar composition: a) 92% – 8%; b) 85% – 15%; c) 60% – 40%. All systems were stained with 18:1 Liss Rhod PE (0.8%) and BODIPY-copolymer (0.02%). More pictures are reported in the Supporting Information (Figure S13).

When the percentage of copolymer increased, the length of the domains where it was present seemed to increase accordingly (Figure 3 b), until a homogeneous distribution of lipids and copolymers in the membrane was attained when the concentration of latter was around 40 mol%, as shown in Figure 3 c). It is worth noting that mixed vesicles were obtained in presence of the same amount of Liss Rhod PE (0.8%) and BODIPY-copolymer (0.02%) for all the investigated compositions. At very low concentration of copolymer 5 (8%), image 3 a) shows the prevailing presence of POPC as stained by Liss Rhod PE while, increasing the copolymer amount, the images 3 b) and 3 c) show an increase in homogeneity of the membrane with consequent

overlapping of both the probes. The increasing spreading of BODIPY-copolymer in the membrane, despite its fixed concentration, demonstrates both the presence of the copolymer into the membrane and the prevailing affinity of the fluorescent copolymer for copolymer-rich regions. Although the membrane composition became more homogeneous at higher copolymer percentages, the total number of stable vesicles detected in the samples drastically diminished, until amphiphilic structures could not be observed at copolymer amount > ~40 mol%. The concentration dependence of both the lipid/copolymer distribution in the membrane and the successful formation of vesicles might depend on the complex attractive interactions taking place between the two molecules, as observed for a DPPC/PIB_{37}-b-PEO_{48} system [32].

It is interesting to compare our results with those previously reported in the literature concerning POPC-based giant vesicles blended with PBD or PDMS. POPC is a lipid in the fluid state at room temperature and in the case of PBD [13,31], homogeneous hybrid GUVs are formed in a restricted range of composition (i.e. in the region of low and high mole polymer content). In these homogeneous vesicles lipid molecules are dispersed in a "sea" of copolymers and vice versa. This situation is the most energetically favoured. Indeed, apart from the chemical affinity, also the structural compatibility has to be taken into account when dealing with lipid/copolymer GUVs. The thickness of polymer bilayers varies between 5 and 50 nm, while the lipid bilayer is 3-4 nm [20,84], i.e. there is a so called hydrophobic mismatch. As a consequence of this hydrophobic mismatch, in phase separated systems, the copolymer has to distort in order to adjust to the lipid bilayer and avoid as much as possible the contacts with water. This has a high energy cost corresponding to high line tension at lipid-polymer boundary. Then, domain formation is most of the time energetically disfavoured. Interestingly in the case of PDMS triblock copolymers [29], hybrid GUVs were formed in all the weight concentration range and

were homogeneous in the polymer-rich region (till 85 wt % polymer content for 1.5k copolymers, 50 wt% for 3k copolymers), while domain formation was observed at lower polymer content. This phase separation was accompanied by budding and the phase-separated, budded vesicles were not stable and budding degenerated in vesicle fission in the lipid rich region. For molecular weight as high as 5k stable phase separated vesicles could not be observed and pure lipid or pure polymer vesicles were present together with homogeneous structures. Budding phenomena can evolve in fission when the line tension at boundary is higher than the curvature energy associated to bending. The authors concluded that line tension at the lipid-polymer boundary were too high in the case of the 5k copolymers. Besides, the authors stressed that block copolymers with the same molecular weight showed even higher instability towards fission than the triblock structures. As observed for PDMS based copolymers, the copolymer presented here forms homogeneous GUVs at high polymer content. On the contrary domain formation is observed without fission between 24 w % and 42 w % POPC despite their higher hydrophobic mismatch (13.8k compared to 5k in the literature). At these compositions the bending costs associated with budding and fission are still higher than the boundary line energy, so phase separation is still energetically favoured to fission. We speculate that our polymer has a higher T_g than PDMS based ones, and consequently a higher curvature energy.

In a different set of experiments, we investigated the influence of the copolymer on the distribution of the water-soluble fluorescent probe pyranine (structure reported in Figure S14 in the Supporting Information) that was dissolved in the I-solution. This probe is membrane impermeable and in pure POPC vesicles it is firmly confined into the aqueous lumen [85,86] as highlighted in Figure 4 a). However, when the copolymer was present, the pyranine tended to accumulate along the membrane (Figure 4 b). The intensity profiles shown in Figure 4 c) and 4

d) highlight the different distribution of pyranine. In pure POPC vesicles the fluorescence is constant along the line and decreases at the border, in the mixed vesicle, in contrast, two peaks appear in proximity of the membrane where pyranine accumulates.

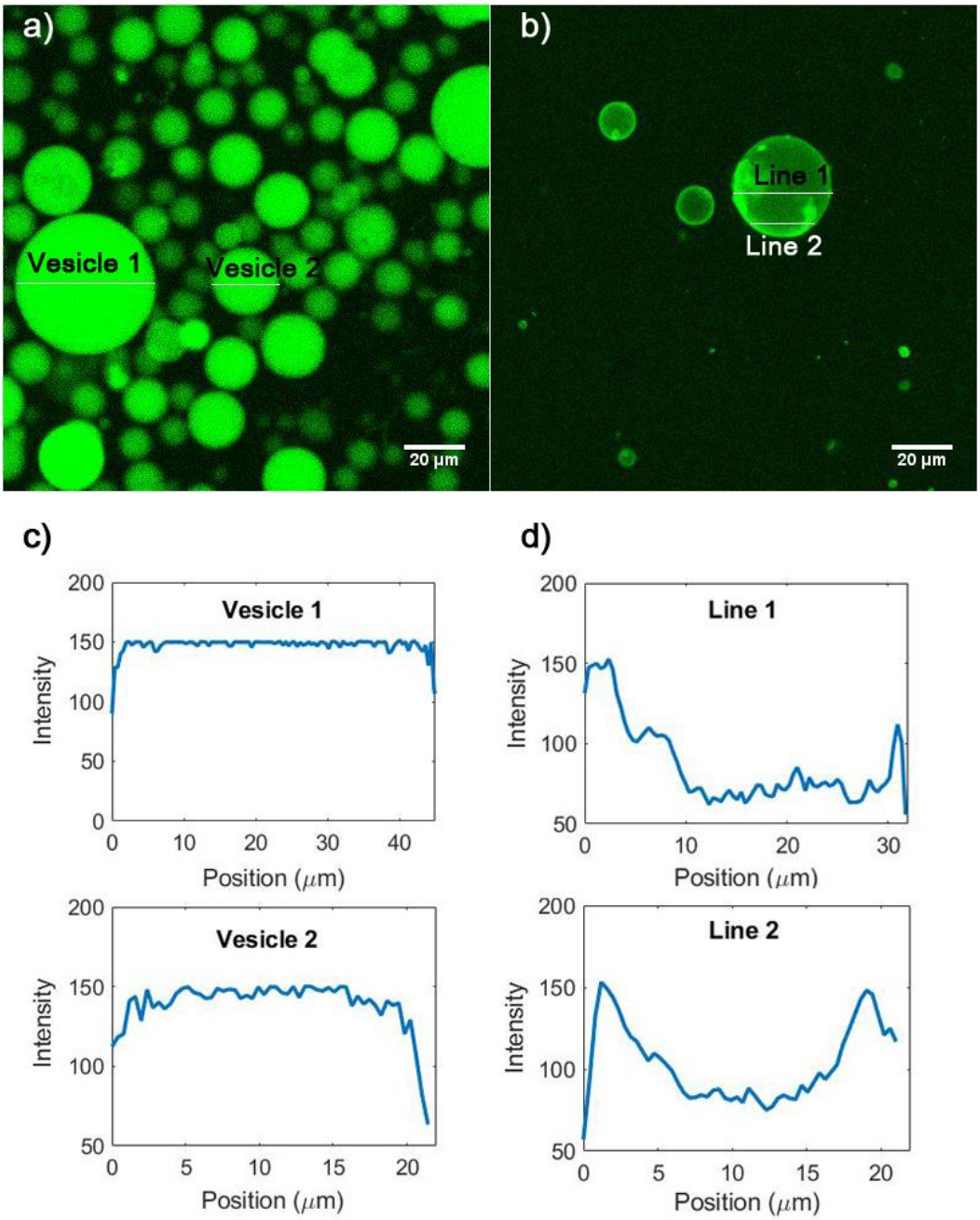

Figure 4 Vesicles made of POPC - copolymer (93% - 7% mol/mol) and pyranine 50 □M. a) Pure POPC vesicles; b) Mixed vesicles; c) Intensity profile taken along a line for vesicles 1 and 2 of Panel a); d) Intensity profile taken along line 1 and line 2 for the vesicle of Panel b).

This behaviour could be attributed to a tendency of pyranine to accumulate in copolymer-rich domains, possibly due to the interaction of its OH moieties with the pH-sensitive units of the

DMAEMA group. This different behaviour observed for pyranine in the absence and in the presence of the copolymer is another proof that the latter is indeed present in the POPC double layer.

CONCLUSION

Hybrid lipid vesicles incorporating a copolymer with a T_g above room temperature have been presented. Our study shows that electroformation cannot be used for these polymers to efficiently obtain giant vesicles, probably linked to a low mobility in the electroformation conditions. However, a method based on an emulsion phase transfer, so far used for lipids or polymers such as PDMS or PBD has been successfully adapted. This can be preferably applied to polymers compatible with lipids based on their solubility and affinity. For this, the solubility parameter and the HLB value can be used to select appropriate candidates. The method presented here will open up new possibilities to develop hybrid systems with a much larger chemical structure variety, leading to new types of synthetic micro reactors or biomimetic compartments. Possible future developments will therefore be adaptive micro-reactor with catalyst groups fixed to the membrane, or pH-sensitive micro- or nano-reactors or synthetic cells with a controlled permeability versus an external stimulus.

ACKNOWLEDGMENTS

The authors thank COST ACTION CM1304 and ERASMUS+ exchange program for funding the mobility of Y.M. from the University of Salerno to the University of Toulouse “Paul Sabatier” and the EU (FEDER-35477 “Nano-objets pour la biotechnologie”) for financial support. Thanks are due to Dr.Patrizia Iannece (University of Salerno) for ESI-MS spectral measurements and Dr. Patrizia Oliva (University of Salerno) for the bidimensional NMR spectral measurements and Dr Stephanie Dauvillier (IPBS, University of Toulouse and CNRS) for assistance with confocal microscope. L.I. thanks Università degli Studi dell’Insubria for the funding granted via “Fondo dell’Ateneo per la Ricerca” (FAR 2018).

LIST OF ABBREVIATIONS

Monomethoxypoly(ethyleneglycol)	mPEG
Poly(ethylene glycol) methyl ether 2-bromoisobutyrate	mPEG-Br
2,2′-Bipyridyl	bpy
1-palmitoyl-2-oleoyl-*sn*-glycero-3-phosphocholine	POPC
1,2-dioleoyl-s*n*-glycero-3-phosphoethanolamine-N-(lissamine rhodamine B sulfonyl) (ammonium salt)	18:1 Liss Rhod PE
Methylmetacrylate	MMA
N,N-(dimethylamino)ethyl methacrylate	DMAEMA
2,6-diethyl-1,3,5,7-tetramethyl-8-[4-[8-(2-methacryloylethyl)dimethylammoniumbromideoctyloxy]phenyl]-4,4'-difluoroboradiaza indacene	BODIPY-DMAEMA
fluorescent mPEG-*block*-P(MMA-*grad*-DMAEMA)	BODIPY-copolymer

ASSOCIATED CONTENT

Supplementary information is available. It describes the characterization of the products in more details and report more pictures about hybrid GUVs.

REFERENCES

[1] F. Meng, Z. Zhong, J. Feijen, Stimuli-responsive polymersomes for programmed drug delivery, Biomacromolecules, 10 (2009) 197–209.

[2] M. Huo, J. Yuan, L. Tao, Y. Wei, Redox-responsive polymers for drug delivery: from molecular design to applications, Polym. Chem., 5 (2014) 1519–1528.

[3] L. Messager, J. Gaitzsch, L. Chierico, G. Battaglia, Novel aspects of encapsulation and delivery using polymersomes, Curr. Opin. Pharmacol., 18 (2014) 104–111.

[4] M. Li, C. Du, N. Guo, Y. Teng, X. Meng, H. Sun, S. Li, P. Yu, H. Galons, Composition design and medical application of liposomes, Eur. J. Med. Chem., (2019).

[5] H. Che, J.C.M. van Hest, Adaptive Polymersome Nanoreactors, ChemNanoMat, 5 (2019) 1092–1109.

[6] I. Louzao, J.C. van Hest, Permeability effects on the efficiency of antioxidant nanoreactors, Biomacromolecules, 14 (2013) 2364–2372.

[7] K. Langowska, C.G. Palivan, W. Meier, Polymer nanoreactors shown to produce and release antibiotics locally, Chem. Commun., 49 (2013) 128–130.

[8] X. Liu, D. Appelhans, B. Voit, Hollow Capsules with Multiresponsive Valves for Controlled Enzymatic Reactions, J. Am. Chem. Soc., 140 (2018) 16106–16114.

[9] O. Rifaie-Graham, S. Ulrich, N.F. Galensowske, S. Balog, M. Chami, D. Rentsch, J.R. Hemmer, J. Read de Alaniz, L.F. Boesel, N. Bruns, Wavelength-selective light-responsive DASA-functionalized polymersome nanoreactors, J. Am. Chem. Soc., 140 (2018) 8027–8036.

[10] Q. Yan, J. Wang, Y. Yin, J. Yuan, Breathing polymersomes: CO2-tuning membrane permeability for size-selective release, separation, and reaction, Angew. Chem. Int. Ed., 52 (2013) 5070–5073.

[11] M. Mohammadi, S. Taghavi, K. Abnous, S.M. Taghdisi, M. Ramezani, M. Alibolandi, Hybrid Vesicular Drug Delivery Systems for Cancer Therapeutics, Adv. Funct. Mater., 28 (2018) 1802136.

[12] W. Shen, J. Hu, X. Hu, Impact of amphiphilic triblock copolymers on stability and permeability of phospholipid/polymer hybrid vesicles, Chem. Phys. Lett., 600 (2014) 56–61.

[13] S.K. Lim, H.-P. de Hoog, A.N. Parikh, M. Nallani, B. Liedberg, Hybrid, Nanoscale Phospholipid/Block Copolymer Vesicles, Polymers, 5 (2013) 1102–1114.

[14] M. Mumtaz Virk, E. Reimhult, Phospholipase A2-induced degradation and release from lipid-containing polymersomes, Langmuir, 34 (2017) 395–405.

[15] Z. Cheng, D.R. Elias, N.P. Kamat, E.D. Johnston, A. Poloukhtine, V. Popik, D.A. Hammer, A. Tsourkas, Improved Tumor Targeting of Polymer-Based Nanovesicles Using Polymer–Lipid Blends, Bioconjug. Chem., 22 (2011) 2021–2029.

[16] W. Zong, B. Thingholm, F. Itel, P.S. Schattling, E. Brodszkij, D. Mayer, S. Stenger, K.N. Goldie, X. Han, B. Städler, Phospholipid–Block Copolymer Hybrid Vesicles with Lysosomal Escape Ability, Langmuir, 34 (2018) 6874–6886.

[17] E. Rideau, R. Dimova, P. Schwille, F.R. Wurm, K. Landfester, Liposomes and polymersomes: a comparative review towards cell mimicking, Chem. Soc. Rev., 47 (2018) 8572–8610.

[18] C. G. Palivan, R. Goers, A. Najer, X. Zhang, A. Car, W. Meier, Bioinspired polymer vesicles and membranes for biological and medical applications, Chem. Soc. Rev., 45 (2016) 377–411.

[19] M. Schulz, W.H. Binder, Mixed Hybrid Lipid/Polymer Vesicles as a Novel Membrane Platform, Macromol. Rapid Commun., 36 (2015) 2031–2041.

[20] J.-F. Le Meins, C. Schatz, S. Lecommandoux, O. Sandre, Hybrid polymer/lipid vesicles: state of the art and future perspectives, Mater. Today, 16 (2013) 397–402.

[21] A. Peyret, E. Ibarboure, J.-F. Le Meins, S. Lecommandoux, Asymmetric hybrid polymer–lipid giant vesicles as cell membrane mimics, Adv. Sci., 5 (2018) 1700453.

[22] M. Bieligmeyer, F. Artukovic, S. Nussberger, T. Hirth, T. Schiestel, M. Müller, Reconstitution of the membrane protein OmpF into biomimetic block copolymer–phospholipid hybrid membranes, Beilstein J. Nanotechnol., 7 (2016) 881–892.

[23] M. Schulz, S. Werner, K. Bacia, W.H. Binder, Controlling molecular recognition with lipid/polymer domains in vesicle membranes, Angew. Chem. Int. Ed., 52 (2013) 1829–1833.

[24] J. Kowal, D. Wu, V. Mikhalevich, C.G. Palivan, W. Meier, Hybrid Polymer–Lipid Films as Platforms for Directed Membrane Protein Insertion, Langmuir, 31 (2015) 4868–4877.

[25] L. Otrin, N. Marušič, C. Bednarz, T. Vidaković-Koch, I. Lieberwirth, K. Landfester, K. Sundmacher, Toward artificial mitochondrion: mimicking oxidative phosphorylation in polymer and hybrid membranes, Nano Lett., 17 (2017) 6816–6821.

[26] R.J.R.W. Peters, M. Marguet, S. Marais, M.W. Fraaije, J.C.M. van Hest, S. Lecommandoux, Cascade Reactions in Multicompartmentalized Polymersomes, Angew. Chem. Int. Ed., 53 (2014) 146–150.

[27] J. Nam, T. Kyle Vanderlick, P. A. Beales, Formation and dissolution of phospholipid domains with varying textures in hybrid lipo-polymersomes, Soft Matter, 8 (2012) 7982–7988.

[28] T.P.T. Dao, F. Fernandes, M. Fauquignon, E. Ibarboure, M. Prieto, J.F.L. Meins, The combination of block copolymers and phospholipids to form giant hybrid unilamellar vesicles (GHUVs) does not systematically lead to “intermediate” membrane properties, Soft Matter, 14 (2018) 6476–6484.

[29] T.P.T. Dao, F. Fernandes, E. Ibarboure, K. Ferji, M. Prieto, O. Sandre, J.-F.L. Meins, Modulation of phase separation at the micron scale and nanoscale in giant polymer/lipid hybrid unilamellar vesicles (GHUVs), Soft Matter, 13 (2017) 627–637.

[30] C. Magnani, C. Montis, G. Mangiapia, A.-F. Mingotaud, C. Mingotaud, C. Roux, P. Joseph, D. Berti, B. Lonetti, Hybrid vesicles from lipids and block copolymers: Phase behavior from the micro-to the nano-scale, Colloids Surf. B Biointerfaces, (2018).

[31] J. Nam, P.A. Beales, T.K. Vanderlick, Giant Phospholipid/Block Copolymer Hybrid Vesicles: Mixing Behavior and Domain Formation, Langmuir, 27 (2011) 1–6.

[32] M. Schulz, D. Glatte, A. Meister, P. Scholtysek, A. Kerth, A. Blume, K. Bacia, W.H. Binder, Hybrid lipid/polymer giant unilamellar vesicles: effects of incorporated biocompatible PIB–PEO block copolymers on vesicle properties, Soft Matter, 7 (2011) 8100–8110.

[33] A. Kubilis, A. Abdulkarim, A.M. Eissa, N.R. Cameron, Giant polymersome protocells dock with virus particle mimics via multivalent glycan-lectin interactions, Sci. Rep., 6 (2016) 32414.

[34] E. Rideau, F.R. Wurm, K. Landfester, Self-Assembly of Giant Unilamellar Vesicles by Film Hydration Methodologies, Adv. Biosyst., 3 (2019) 1800324.

[35] M.I. Angelova, D.S. Dimitrov, Liposome electroformation, Faraday Discuss. Chem. Soc., 81 (1986) 303–311.

[36] B.M. Discher, Y.-Y. Won, D.S. Ege, J.C.-M. Lee, F.S. Bates, D.E. Discher, D.A. Hammer, Polymersomes: Tough Vesicles Made from Diblock Copolymers, Science, 284 (1999) 1143–1146.

[37] M. Dionzou, A. Morere, C. Roux, B. Lonetti, J.-D. Marty, C. Mingotaud, P. Joseph, D. Goudouneche, B. Payre, M. Leonetti, A.-F. Mingotaud, Comparison of methods for the fabrication and the characterization of polymer self-assemblies: what are the important parameters, Soft Matter, 12 (2016) 2166–2176.

[38] A.M. Eissa, M.J. Smith, A. Kubilis, J.A. Mosely, N.R. Cameron, Polymersome-forming amphiphilic glycosylated polymers: Synthesis and characterization, J. Polym. Sci. Part Polym. Chem., 51 (2013) 5184–5193.

[39] J.P. Reeves, R.M. Dowben, Formation and properties of thin-walled phospholipid vesicles, J. Cell. Physiol., 73 (1969) 49–60.

[40] R. Dimova, U. Seifert, B. Pouligny, S. Förster, H.-G. Dobereiner, Hyperviscous diblock copolymer vesicles, Eur. Phys. J. E, 7 (2002) 241–250.

[41] Y. Zhou, D. Yan, Real-Time Membrane Fission of Giant Polymer Vesicles, Angew. Chem. Int. Ed., 44 (2005) 3223–3226.

[42] E. Rideau, F.R. Wurm, K. Landfester, Giant polymersomes from non-assisted film hydration of phosphate-based block copolymers, Polym. Chem., 9 (2018) 5385–5394.

[43] A. Weinberger, F.-C. Tsai, G.H. Koenderink, T.F. Schmidt, R. Itri, W. Meier, T. Schmatko, A. Schröder, C. Marques, Gel-Assisted Formation of Giant Unilamellar Vesicles, Biophys. J., 105 (2013) 154–164.

[44] K.S. Horger, D.J. Estes, R. Capone, M. Mayer, Films of Agarose Enable Rapid Formation of Giant Liposomes in Solutions of Physiologic Ionic Strength, J. Am. Chem. Soc., 131 (2009) 1810–1819.

[45] T.P.T. Dao, M. Fauquignon, F. Fernandes, E. Ibarboure, A. Vax, M. Prieto, J.-F. Le Meins, Membrane properties of giant polymer and lipid vesicles obtained by electroformation and PVA gel-assisted hydration methods, Colloids Surf. Physicochem. Eng. Asp., 533 (2017) 347–353.

[46] S. Pautot, B.J. Frisken, D.A. Weitz, Production of Unilamellar Vesicles Using an Inverted Emulsion, Langmuir, 19 (2003) 2870–2879.

[47] C. Martino, A.J. deMello, Droplet-based microfluidics for artificial cell generation: a brief review, Interface Focus, 6 (2016) 20160011.

[48] S. Deshpande, C. Dekker, On-chip microfluidic production of cell-sized liposomes, Nat. Protoc., 13 (2018) 856–874.

[49] M. Abkarian, E. Loiseau, G. Massiera, Continuous droplet interface crossing encapsulation (cDICE) for high throughput monodisperse vesicle design, Soft Matter, 7 (2011) 4610–4614.

[50] M.C. Blosser, B.G. Horst, S.L. Keller, cDICE method produces giant lipid vesicles under physiological conditions of charged lipids and ionic solutions, Soft Matter, 12 (2016) 7364–7371.

[51] K. Dürre, A.R. Bausch, Formation of phase separated vesicles by double layer cDICE, Soft Matter, (2019).

[52] J. Petit, I. Polenz, J.-C. Baret, S. Herminghaus, O. Bäumchen, Vesicles-on-a-chip: A universal microfluidic platform for the assembly of liposomes and polymersomes, Eur. Phys. J. E, 39 (2016) 59.

[53] K. Kamiya, R. Kawano, T. Osaki, K. Akiyoshi, S. Takeuchi, Cell-sized asymmetric lipid vesicles facilitate the investigation of asymmetric membranes, Nat. Chem., 8 (2016) 881–889.

[54] A. Moga, N. Yandrapalli, R. Dimova, T. Robinson, Optimization of the Inverted Emulsion Method for High-Yield Production of Biomimetic Giant Unilamellar Vesicles, ChemBioChem, 20 (2019) 2674–2682.

[55] H. Che, S. Cao, J.C.M. van Hest, Feedback-Induced Temporal Control of "Breathing" Polymersomes To Create Self-Adaptive Nanoreactors, J. Am. Chem. Soc., 140 (2018) 5356–5359.

[56] S. Villani, R. Adami, E. Reverchon, A.M. Ferretti, A. Ponti, M. Lepretti, I. Caputo, L. Izzo, pH-sensitive polymersomes: controlling swelling via copolymer structure and chemical composition, J. Drug Target., 25 (2017) 899–909.

[57] E. Yoshida, pH response behavior of giant vesicles comprised of amphiphilic poly (methacrylic acid)-block-poly (methyl methacrylate-random-mathacrylic acid), Colloid Polym. Sci., 293 (2015) 649–653.

[58] E. Yoshida, Giant vesicles comprised of mixed amphiphilic poly (methacrylic acid)-block-poly (methyl methacrylate-random-methacrylic acid) diblock copolymers, Colloid Polym. Sci., 293 (2015) 3641–3648.

[59] E. Yoshida, Preparation of giant vesicles containing quaternary ammonium salt of 2-(dimethylamino) ethyl methacrylate through photo nitroxide-mediated controlled/living radical polymerization-induced self-assembly, J. Polym. Res., 25 (2018) 109.

[60] K. Sreenath, R.J. Clark, L. Zhu, Tricolor emission of a fluorescent heteroditopic ligand over a concentration gradient of zinc (II) ions, J. Org. Chem., 77 (2012) 8268–8279.

[61] S. Matrella, C. Vitiello, M. Mella, G. Vigliotta, L. Izzo, The Role of Charge Density and Hydrophobicity on the Biocidal Properties of Self-Protonable Polymeric Materials, Macromol. Biosci., 15 (2015) 927–940.

[62] M. Manunta, L. Izzo, R. Duncan, A.T. Jones, Establishment of subcellular fractionation techniques to monitor the intracellular fate of polymer therapeutics II Identification of endosomal and lysosomal compartments in HepG2 cells combining single-step subcellular fractionation with fluorescent imaging, J. Drug Target., 15 (2007) 37–50.

[63] M. Berna, D. Dalzoppo, G. Pasut, M. Manunta, L. Izzo, A.T. Jones, R. Duncan, F.M. Veronese, Novel monodisperse PEG- dendrons as new tools for targeted drug delivery: synthesis, characterization and cellular uptake, Biomacromolecules, 7 (2006) 146–153.

[64] M.I. Angelova, S. Soléau, Ph. Méléard, F. Faucon, P. Bothorel, Preparation of giant vesicles by external AC electric fields Kinetics and applications, in: C. Helm, M. Lösche, H. Möhwald (Eds.), Trends Colloid Interface Sci. VI, Steinkopff, Darmstadt, 1992: pp. 127–131.

[65] J.H. Hildebrand, R.L. Scott, The Solubility of Non-electrolytes, third edition, Reinhold, New York, 1950.

[66] J.H. Hildebrand, R.L. Scott, Regular Solutions, Prentice-Hall Inc., New Jersey, 1962.

[67] M. Gilbert, Chapter 5 - Relation of Structure to Chemical Properties, in: M. Gilbert (Ed.), Brydsons Plast. Mater. Eighth Ed., Butterworth-Heinemann, 2017: pp. 75–102.

[68] K. Min, H. Gao, K. Matyjaszewski, Use of Ascorbic Acid as Reducing Agent for Synthesis of Well-Defined Polymers by ARGET ATRP, Macromolecules, 40 (2007) 1789–1791.

[69] H. Dong, K. Matyjaszewski, ARGET ATRP of 2-(Dimethylamino)ethylMethacrylate as an Intrinsic Reducing Agent, Macromolecules, 41 (2008) 6868–6870.

[70] A. Tagliabue, L. Izzo, M. Mella, Impact of Charge Correlation, Chain Rigidity, and Chemical Specific Interactions on the Behavior of Weak Polyelectrolytes in Solution, J. Phys. Chem. B, 123 (2019) 8872–8888.

[71] M. Mella, L. Izzo, Modulation of ionization and structural properties of weak polyelectrolytes due to 1D, 2D, and 3D confinement, J. Polym. Sci. Part B Polym. Phys., 55 (2017) 1088–1102.

[72] M. Mella, L. Izzo, Structural properties of hydrophilic polymeric chains bearing covalently–linked hydrophobic substituents: Exploring the effects of chain length, fractional loading and hydrophobic interaction strength with coarse grained potentials and Monte Carlo simulations, Polymer, 51 (2010) 3582–3589.

[73] M. Mella, M.V.L. Rocca, Y. Miele, L. Izzo, On the origin and consequences of high DMAEMA reactivity ratio in ATRP copolymerization with MMA: An experimental and theoretical study#, J. Polym. Sci. Part Polym. Chem., 56 (2018) 1366–1382.

[74] A.S. Klymchenko, R. Kreder, Fluorescent Probes for Lipid Rafts: From Model Membranes to Living Cells, Chem. Biol., 21 (2014) 97–113.

[75] M. Chemin, P.-M. Brun, S. Lecommandoux, O. Sandre, J.-F. Le Meins, Hybrid polymer/lipid vesicles: fine control of the lipid and polymer distribution in the binary membrane, Soft Matter, 8 (2012) 2867–2874.

[76] T. Ruysschaert, A.F.P. Sonnen, T. Haefele, W. Meier, M. Winterhalter, D. Fournier, Hybrid Nanocapsules: Interactions of ABA Block Copolymers with Liposomes, J. Am. Chem. Soc., 127 (2005) 6242–6247.

[77] A. Somasundar, S. Ghosh, F. Mohajerani, L.N. Massenburg, T. Yang, P.S. Cremer, D. Velegol, A. Sen, Positive and negative chemotaxis of enzyme-coated liposome motors, Nat. Nanotechnol., 14 (2019) 1129–1134.

[78] R. Dimova, C. Marques, C. Marques, The Giant Vesicle Book, CRC Press, 2019.

[79] P. Stano, T.P. de Souza, P. Carrara, E. Altamura, E. D'Aguanno, M. Caputo, P.L. Luisi, F. Mavelli, Recent Biophysical Issues About the Preparation of Solute-Filled Lipid Vesicles, Mech. Adv. Mater. Struct., 22 (2015) 748–759.

[80] P. Stano, Minimal cells: relevance and interplay of physical and biochemical factors, Biotechnol. J., 6 (2011) 850–859.

[81] E. Altamura, P. Stano, P. Walde, F. Mavelli, Giant Vesicles as Micro-Sized Enzymatic Reactors: Perspectives and Recent Experimental Advancements, Int. J. Unconv. Comput., 11 (2015) 5–21.

[82] L. Jin, N.P. Kamat, S. Jena, J.W. Szostak, Fatty Acid/Phospholipid Blended Membranes: A Potential Intermediate State in Protocellular Evolution, Small, 14 (2018) 1704077.

[83] P. Carrara, P. Stano, P.L. Luisi, Giant Vesicles "Colonies": A Model for Primitive Cell Communities, ChemBioChem, 13 (2012) 1497–1502.

[84] J.F. Nagle, S. Tristram-Nagle, Structure of lipid bilayers, Biochim. Biophys. Acta, 1469 (2000) 159–195.

[85] Y. Miele, T. Bánsági, A.F. Taylor, P. Stano, F. Rossi, Engineering Enzyme-Driven Dynamic Behaviour in Lipid Vesicles, in: F. Rossi, F. Mavelli, P. Stano, D. Caivano (Eds.), Adv. Artif. Life Evol. Comput. Syst. Chem., Springer International Publishing, Cham, 2016: pp. 197–208.

[86] Y. Miele, Z. Medveczky, G. Hollo, B. Tegze, I. Derenyi, Z. Horvolgyi, E. Altamura, I. Lagzi, F. Rossi, Self-Division of Giant Vesicles Driven by an Internal Enzymatic Reaction, Chem. Sci., in press (2020).